Materiales de Construcción (75) 360
October-December 2025, e393
ISSN-L: 0465-2746, eISSN: 1988-3226
https://doi.org/10.3989/mc.2025.402124

Eco-efficient particle-packing-optimized concrete incorporating supplementary cementitious materials

M. Pastorini Proença [a,d]✉, M. Pastorini Proença [b], M. Batista de Oliveira [a], L.M. Zanette Oliveira [c], D.R. Oliveira Pruner [b,c], H. Fuganti Campos [d], N. Soares Klein [d]

a. Federal Institute of Paraná (Foz do Iguaçu, Brazil)
b. Federal University of Latin American Integration (Foz do Iguaçu, Brazil)
c. Dinâmica das Cataratas University Center (Foz do Iguaçu, Brazil)
d. Federal University of Paraná (Curitiba, Brazil)
✉: melissa.proenca@ifpr.edu.br

Received 23 November 2024
Accepted 06 April 2025
Available on line 10 December 2025

ABSTRACT: The use of supplementary cementitious materials (SCM) is a key to reducing CO_2 emissions in the cement industry. This study analyzed concrete dosed with Alfred's packing model, incorporating waste powders (mixed powder, concrete powder, brick powder, and glass powder) as SCM at replacement levels of 48%, 33%, 42%, and 32%, respectively. Properties such as absorption, voids index, compressive strength, dynamic modulus of elasticity, electrical resistivity, and environmental indexes were evaluated at 28 days. Results showed that brick powder exhibits pozzolanic activity, while the other powders act as fillers. Except for mixed powder concrete, all achieved high-strength concrete status (>50 MPa). All mixtures had negligible corrosion risk and binder and carbon indexes reduced by up to 37% and 35%, respectively. The study highlights the potential of recycled powders to lower emissions and promote circular economy practices.

KEY WORDS: Recycled powder; Eco-efficient concrete; Circular economy; Particle packing; Alfred's model.

Citation/Citar como: Pastorini Proença M, Pastorini Proença M, de Oliveira MB, Zanette Oliveira LM, Oliveira Pruner DR, Fuganti Campos H, Soares Klein N. 2025. Eco-efficient particle-packing-optimized concrete incorporating supplementary cementitious materials. Mater. Construcc. 75(360):e393. https://doi.org/10.3989/mc.2025.402124

RESUMEN: *Hormigón ecoeficiente optimizado por empaquetamiento de partículas que incorpora materiales cementantes suplementarios.* El uso de materiales cementantes suplementarios (MCS) es clave para reducir las emisiones de CO_2 en la industria del cemento. Este estudio evaluó hormigones dosificados con el modelo de empaquetamiento de Alfred, incorporando polvos residuales (mixto, hormigón, de ladrillo y vidrio) como MCS, con niveles de reemplazo del 48%, 33%, 42% y 32%, respectivamente. Se analizaron propiedades como absorción, vacíos, resistencia a la compresión, módulo dinámico de elasticidad, resistividad eléctrica e indicadores ambientales a los 28 días. El polvo de ladrillo mostró actividad puzolánica, mientras que los demás actuaron como rellenos. Todos los hormigones, excepto el de polvo mixto, superaron los 50 MPa, clasificándose como de alta resistencia. Además, todas las mezclas presentaron riesgo de corrosión insignificante y reducciones en los índices de aglutinante y carbono de hasta el 37% y 35%. El estudio destaca el potencial de los polvos reciclados para reducir emisiones y promover la economía circular.

PALABRAS CLAVE: Polvo reciclado; Hormigón ecoeficiente; Economía circular; Empaquetamiento de partículas; Modelo de Alfred.

1. INTRODUCTION

The construction sector development is directly linked to environmental damage due to natural resource extraction and greenhouse gas emissions (1,2). One of the main construction materials with a major environmental impact is Portland cement, with a production process responsible for 5-7% of global CO_2 emissions (3,4). In cement production, obtaining clinker (an essential Portland cement element) has an emission factor of 865 kg of CO_2/tonne of clinker (5); approximately 60% of these emissions occur during the limestone decarbonization chemical process, and the rest is associated with the burning of fuels to reach the clinkerization temperature. (4,6,7).

As a result of the impact linked to the cement industry, cementitious matrices such as concrete and mortar that use Portland cement as an input carry a high emissive potential (8–10) since up to 90% of concrete emissions may come specifically from Portland cement (11). Portland cement demand estimates for 2050, considering the need for infrastructure and population growth (12), would increase from 4 to 6 billion tons worldwide (13,14). Still, for 2050, the goal is to achieve the NetZero scenario, where CO_2 emissions from a product or process would be offset by a direct CO_2 emissions reduction or avoided emissions (7,15). In this sense, the use of supplementary cementitious materials (SCM) would be one of the key alternatives for carbon emissions reduction in the cement industry (4,11,16,17). They are usually waste materials from other production chains (9,11,18,19), which, when finely comminuted, act on the pozzolanic reaction and the filler effect (16,20).

SCM allows for the CO_2 emission reduction, also promoting the circular economy within the construction industry (21–23) since it uses construction and demolition waste, such as ceramic materials (9,24,25), concrete (21,26), mixed residue (27,28), and also waste from other sectors such as glass powder (19,29).

Another way to help reduce the carbon footprint associated with cementitious matrices is to use techniques that improve the materials' application (15). In this sense, particle packing allows for the materials' proper mix-design considering the granular distribution of the whole set of particles, thus optimizing Portland cement consumption and reducing carbon emissions (30–33). One of the most well-known particle packing models is the modified Andreasen and Andersen model (also known as Alfred model), proposed by Funk and Dinger (1994) (32).

In this context, this study aims to evaluate the performance of concretes designed using the Alfred model, incorporating different SCM of residual origin: glass powder, ceramic powder, concrete powder, and mixed powder. The environmental parameters of carbon and binder indexes, and the mechanical and durability properties were verified, seeking to understand the potential use of the SCM, combined with the optimization proportion of concrete mixtures.

2. MATERIALS AND METHODS

2.1. Materials

Portland cement CP V ARI (high initial strength Portland cement), equivalent to ASTM C 150/C150M Type III, was used to produce the concretes, as it has the highest clinker content among the commercial cement recommended by NBR 16697. (35). To ensure the concrete workability, with a low water/fines ratio, a third-generation polycarboxylate-based superplasticizing additive (SP) with a 1.1 g/cm³ specific mass was used following NBR 11768 (36). Its content was determined by analyzing the saturation point using the Kantro cone (37).

The supplementary cementitious materials used in the compositions were mixed powder (MP) from construction and demolition waste (CDW) sand. Concrete powder (CP) from residual concrete, test specimens. Brick powder (BP) from CDW ceramic brick. Glass powder (GP) from glass beverage bottles. Figure 1 represents the sources of the SCM used in this study, as well as the classification according to the composition as per NBR 15116 (38).

Classification - CDW NBR 15116 [38]	Mixed powder	Concrete powder	Brick powder	Glass powder
Cement paste fragments (%)	50,62	86,01	0	0
Rock fragments (%)	11,62	13,99	0	0
Fragments of red ceramic (%)	29,66	0	100	0
Fragments of plaster, metals, plastic, glass, organics (%)	8,10	0	0	100*

*100% Glass

Figure 1. Sources of the SCM.

Table 1. Aggregates Physical Properties.

Properties	Gravel 12.5	Gravel 19	Sand	Cement	CP	MP	GP	BP
Specific mass (Kg/m³)	2870	2870	2660	3020	2470	2560	2550	2660
Maximum size (mm)	12.5	19	2.39	_	_	_	_	_
Fineness modulus (mm)	_	_	2.2	_	_	_	_	_
d50 (μm)	6300	12500	300	11.94	21.03	22.19	34.25	20.85

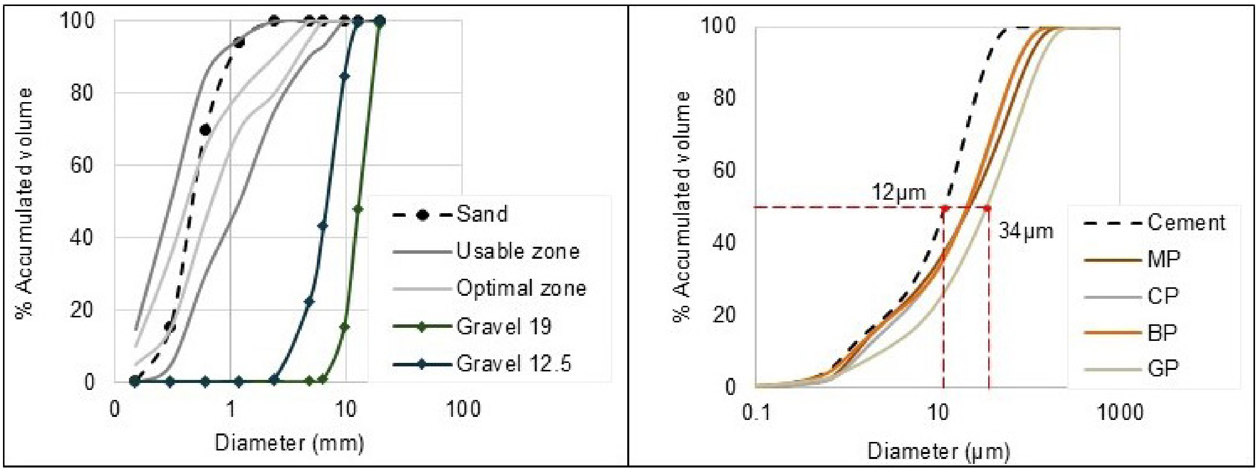

a) Aggregates b) Recycled powders

Figure 2. Particle size distribution (PSD).

The aggregates used were natural river sand and basaltic gravel of maximum sizes 12.5 and 19 mm, as shown in Table 1 and Figure 2a. Table 1 and Figure 2b show the powders' physical characteristics.

2.2. Methods

The methods were divided into powder reactivity analysis, and their performance was tested when applied as SCM in concrete.

2.2.1. SCM chemical composition and reactivity

The chemical characterization of SCM was performed by X-ray fluorescence (XRF) carried out using a Bruker S8 Tiger spectrometer, with loss on ignition determination. For X-ray diffraction (XRD), a Panalytical diffractometer was used, with Cu Kα radiation and λ = 1.5418 Å in spin mode, and the diffractograms were analyzed using Panalytical's X'Pert High Score Plus V4.8 software and compared with standards from the COD (Crystallography Open Database). SCM reactivity was assessed using the indirect lime activity method at 7 days according to NBR 5752 (39), performance index with Portland cement at 28 days following the NBR 5751 (40), and also by the calcium hydroxide consumption by the modified Chapelle method according to NBR 15895 (41).

2.2.2. Concrete mix-design, production and characterization

To analyze SCM-packed concretes, defining the distribution modulus q is first necessary. It dictates the concrete matrix's granular composition and the mixtures' workability (42–44). The lower the q value, the greater the amount of fine particles (44). The distribution modulus q of 0.37 is recommended in the literature to obtain the maximum packing density (45), and values below this tend to maintain the packing condition with an increased amount of fine particles. However, it is important to calibrate the distribution modulus q for the different aggregates and grain types used in the mixtures (44). The aggregates' shape, the specific surface area, and the particle size distribution must be considered (43). Preliminary analysis in this study showed that a q value of 0.37 lead to a high consumption of coarse aggregates and lack of paste to fill the voids between the gravel particles. Thus q values of 0.27 and 0.17 were tested, compatible with the studies by Hunger (2010) and Lopes, Peçanha, and Castro

(2020) (43,46). For concretes with SCM, q= 0.17 was used to maximize the incorporation of fines in the mixes. The concretes were then dosed using Alfred model proposed by Funk and Dinger (1994) (34) as per Equation [1].

$$CPFT = \frac{D^q - D^q_{min}}{D^q_{máx} - D^q_{min}} \quad [1]$$

Where: CPFT = Cumulative % (volume) finer than D; D = Particle diameter (sieve openings) (mm); D_{min} = Minimum diameter, smallest particle in the mixture (mm); D_{max} = Maximum diameter, largest particle in the mixture (mm); q = Distribution modulus.

The ratios of each granular material in the concrete composition were adjusted until the concrete particle size distribution was close to Alfred model's target curve. We used a convergence algorithm based on the Minimum Squares Method associated with the Monte Carlo method developed by Mercuri (2023) (47). A similar approach was adopted by Christófolli et al. (2025) (48). When the deviation between the concrete particle size distribution and the theoretical packing curve (Alfred model) is minimal, represented by the sum of the residual squares as per Equation [2] (49), the packing is optimized.

$$RSS = \sum_{i=1}^{n}\left(CPFT_{mix}\left(D_i^{i+1}\right) - CPFT_{alfred}\left(D_i^{i+1}\right)\right)^2 \quad [2]$$

Where: RSS = Residual sum of squares; $CPFT_{mix}$ = Cumulative percentage (volume) finer than D for the concrete mixture; $CPFT_{alfred}$ = Cumulative percentage (volume) finer than D for Alfred model; D = Particle diameter (sieve openings) (mm).

The experimental flowchart for this stage is shown in Figure 3. The concrete slump class was kept at S160 (pumpable concrete) (50), and the amount of water in the mixture was defined as that enough to meet the slump test. The water content is expressed in Tables 2 and 3 as the water/cement ratio (w/c), and the water/fines ratio (w/f) according to the proportion of fines (cement + SCM).

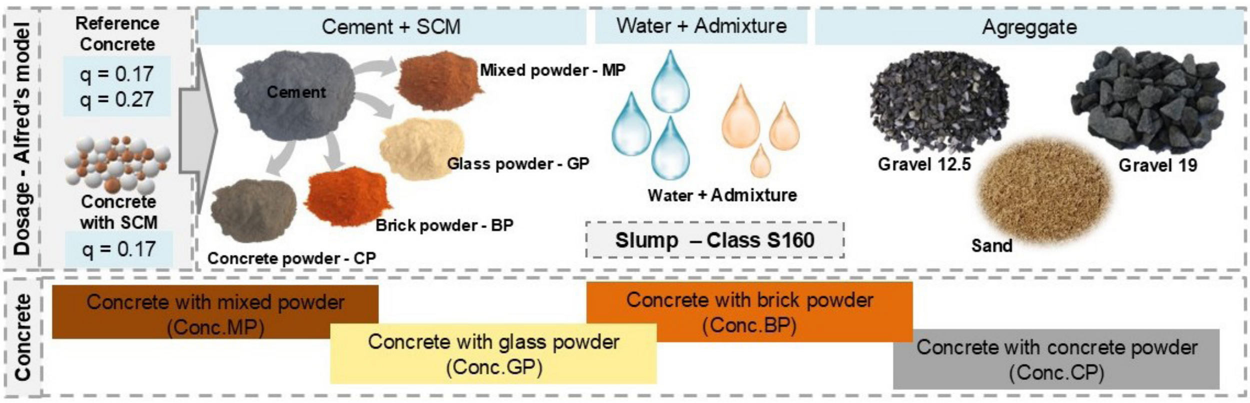

Figure 3. Experimental project.

Materials quantification for concrete production is shown in Tables 2 and 3. It is possible to observe in Table 3 that even though all concretes were designed with the same value for q, the composition between concretes vary due to the different PSD and specific masses of the SCM. This is because Alfred model delivers results of materials proportion in volume, not mass. It is also because different SCM were used in each concrete, so when the volume is converted to mass, values differ from one concrete to the other. The intrinsic characteristics of the SCM, such as PSD, also lead to different contents for cement substitution. However, the PSD curve of these concretes is optimized considering all materials (including cement, SCM, fine and coarse aggregate). In this sense, the comparisons are made using a material (concrete) with a similar granular arrangement, but with SCM from different sources, seeking to compare the potential of using these different SCM.

The concrete mixing procedure was based on that proposed by Damineli (2013)(51) and Campos (2019)(52). Fifteen cylindrical specimens 100 mm in diameter and 200 mm high were produced for each type of concrete. Compaction was carried out manually with a densifying rod in two layers of 12 strokes, according to NBR 5738 (53). In the fresh state, the concrete slump was checked using the slump test according to the NBR 16889 (54) to maintain the slump in class S160 (pumpable concrete) (50).

Table 2. Reference concrete materials consumption.

			Materials	Cement	Sand	Gravel 12.5	Gravel 19	w/c ratio	SP
Reference concrete	q=0.27	REF 0.27	% volume	13.59	29.54	21.84	35.03		
			Proportion	1.00	1.91	1.53	2.45	0.40	0.9%
			Consumption (kg/m³)	352.61	674.89	538.42	863.52	141.04	3.17
	q=0.17	REF 0.17	Materials	Cement	Sand	Gravel 12.5	Gravel 19	w/c	SP
			% volume	22.08	31.64	20.18	26.11		
			Proportion	1.00	1.26	0.87	1.12	0.40	0.9%
			Consumption (kg/m³)	526.33	664.37	457.20	591.56	210.53	4.74

Table 3. Concretes with SCM materials consumption.

		Materials	Cement	MP	Sand	Gravel 12.5	Gravel 19	w/f[1]	SP
q =0.17	Concrete with mixed powder (Conc.MP)	% volume	11.06	11.98	30.98	19.90	26.08		
		Proportion	0.52	0.48	1.29	0.89	1.17	0.31	0.9%
		Consumption (kg/m³)	265.76	244.21	656.00	454.52	595.91	160.56	4.59
	Concrete with glass powder (Conc.GP)	**Materials**	**Cement**	**GP**	**Sand**	**Gravel 12.5**	**Gravel 19**	**w/f**	**SP**
		% volume	15.62	8.71	29.71	20.73	25.23		
		Proportion	0.68	0.32	1.14	0.86	1.04	0.30	0.9%
		Consumption (kg/m³)	369.30	173.86	618.49	465.76	566.73	162.95	4.89
	Concrete with brick powder (Conc.BP)	**Materials**	**Cement**	**BP**	**Sand**	**Gravel 12.5**	**Gravel 19**	**w/f**	**SP**
		% volume	12.51	10.78	30.52	19.15	27.04		
		Proportion	0.57	0.43	1.22	0.83	1.17	0.39	1.2%
		Consumption (kg/m³)	298.44	226.60	641.26	434.27	613.00	202.60	4.73
	Concrete with concrete powder (Conc.CP)	**Materials**	**Cement**	**CP**	**Sand**	**Gravel 12.5**	**Gravel 19**	**w/f**	**SP**
		% volume	14.46	8.87	30.67	19.39	26.60		
		Proportion	0.67	0.33	1.24	0.85	1.16	0.36	0.8%
		Consumption (kg/m³)	345.98	173.63	646.33	440.94	604.65	185.33	4.68

[1]w/f = water/fines ratio

In the hardened state, water absorption and the voids index were evaluated following NBR 9778 (55) at 28 days and compressive strength at 28 and 180 days (56) in a Contenco model I-3025-B digital electric press with a 100 T capacity. The analysis of variance was performed using the Tukey test, with a significance level of 0.05. Letters corresponding to the classification were added to the results graphs, therefore all concretes indicated with the same letter are statistically equal according to the analysis of variance.

The Wenner method (1915) was used for the surface electrical resistivity test, carried out using Proceq Resipod equipment, with a 40 Hz frequency and a 10 µA to 200 µA current. The spacing between the four electrodes was 5 cm. Three samples were used per type of concrete, and three readings were taken on three sides of the specimens at 28 days, following the UNE 83988-2 standard procedures (57).

The concrete environmental performance analysis was based on Damineli et al. (2010) (58), with the binder index (BI) being the ratio between cement consumption and compressive strength at 28 days, according to Equation [3].

$$BI = \frac{Ccem}{fc} \qquad [3]$$

Where: *BI* = Binder index (kg/m³ of cement/MPa); *Ccem* = Portland cement consumption (kg/m³); *fc* = compressive strength (MPa).

For the carbon index (CI), it was necessary to inventory the carbon emissions in kg of CO_2/m^3 of concrete (Equation [4]) and then obtain the index as a function of the compressive strength, according to (Equation [5]).

$$E = (E_{Cem} * C_{Cem}) + (E_{Sand} * C_{Sand}) + (E_{Gravel} * C_{Gravel}) + (E_{SP} * C_{SP}) \quad [4]$$

$$CI = \frac{E}{fc} \quad [5]$$

Where: E = Concrete emission (kg of CO_2/m^3); E_{Cem} = Cement emission (kg of CO_2/kg); C_{Cem} = Cement consumption (kg/m³); E_{Sand} = Sand emission (kg of CO_2/kg); C_{Sand} = Sand consumption (kg/m³); E_{Gravel}= Gravel emission (kg of CO_2/kg); C_{Gravel} = Gravel consumption (kg/m³); E_{SP} = superplasticizer emission (kg of CO_2/kg); C_{SP}= superplasticizer consumption (kg/m³); CI = Carbon index (kg/m³ of CO_2/MPa).

The cement, sand, and gravel emissions (Table 4) were obtained from the Construction Environmental Performance Information System (SIDAC, 2024) (60), while the superplasticizers emissions data were adopted from the Environmental Product Declaration (EFCA, 2021) (61). For CDW powders, the emissions from CDW processing were considered as per Oliveira (2022) (59).

Table 4. Carbon Emissions Data.

CO_2 Emissions		Source	Kg·CO_2/Kg
SCM	Concrete powder (CP)	(59)	0,049
	Mixed powder (MP)		0,049
	Brick powder (BP)		0,025
	Glass powder (GP)		0,049
Cement		(60)	0,776
Superplasticizer		(61)	1,53
Natural fine aggregate		(60)	0,013
Natural coarse aggregate		(60)	0,005

3. RESULTS AND DISCUSSION

3.1. SCM reactivity and chemical composition

In the analysis of the mineralogical composition by X-ray diffraction (Figure 4), no crystalline peaks were identified in the diffractogram for the glass powder (GP), with a predominantly silica and sodium dioxide composition (due to the origin of the soda-lime glass), this condition indicates an amorphous material (62,63). In the brick powder, silica peaks predominate, also as verified by Brekailo et al. (2019) and Hoppe Filho et al. (2021) (24,64). The concrete powder presented peaks of carbonate, silica, portlandite and calcite; these minerals come from the composition of concrete and mortar (65,66). In the mixed powder, there is a predominance of silica, dolomite, calcium carbonate and labratorite (feldspar) peaks; it also presents compositions of ceramics, concrete and mortar.

The supplementary cementitious materials reactivity analysis showed (Figure 5) that mixed powder (MP), and ceramic powder (BP) had the highest performance index with cement at 28 days. In contrast, concrete powder (CP) and glass powder (GP) did not meet the minimum 90% requirement set by NBR 12653 (67). In the 7-day lime activity, BP was the only one to meet the strength requirement of more than 6 MPa, corroborating a higher calcium hydroxide (805 mg$Ca(OH)_2$/g of material) consumption in the modified Chapelle test.

The pozzolanic reaction depends on the material containing silica and alumina in amorphous phases reacting with the calcium hydroxide in the cement matrix to form C-S-H (hydrated calcium silicates) and C-A-S-H (hydrated calcium aluminate silicates) (68,69). Considering the materials' origin, a higher silica and alumina content is expected in the ceramic bricks (BP). According to the x-ray fluorescence analysis, the ceramic brick powder (BP) has a silica, alumina and ferrite content higher than 91%, meeting the chemical requirement for pozzolans according to NBR 12653 (67). Although the glass powder has greater activity with lime and calcium hydroxide consumption than CP and MP, it cannot be classified as pozzolan. Thus, GP, MP and CP contribute to the physical effect of filling the microstructure.

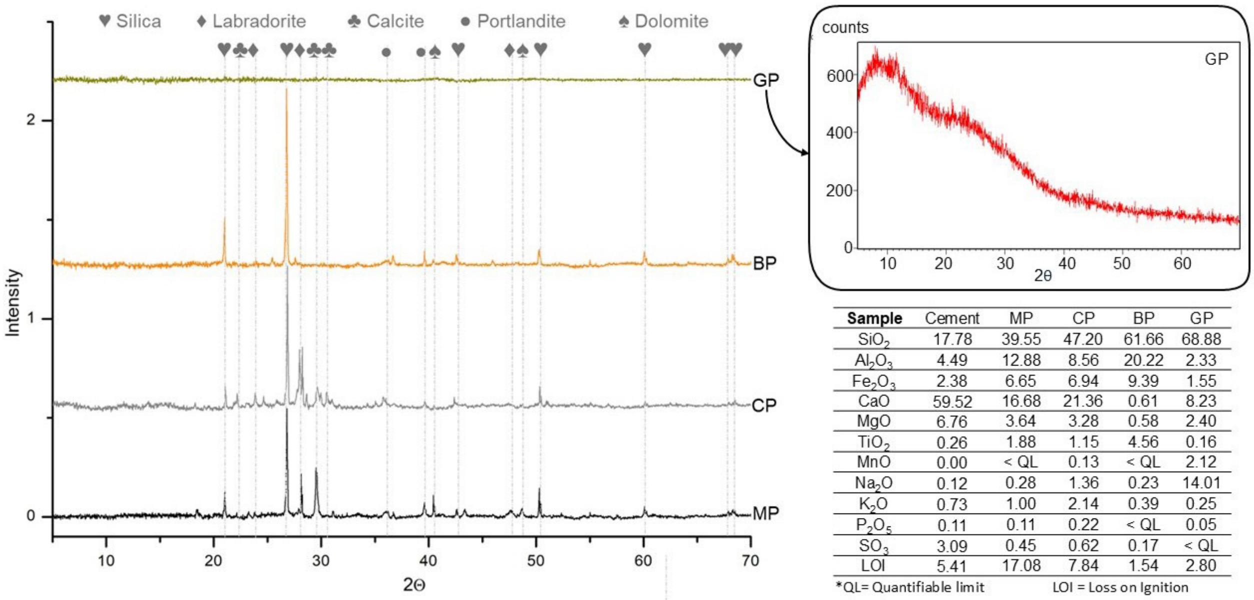

Sample	Cement	MP	CP	BP	GP
SiO_2	17.78	39.55	47.20	61.66	68.88
Al_2O_3	4.49	12.88	8.56	20.22	2.33
Fe_2O_3	2.38	6.65	6.94	9.39	1.55
CaO	59.52	16.68	21.36	0.61	8.23
MgO	6.76	3.64	3.28	0.58	2.40
TiO_2	0.26	1.88	1.15	4.56	0.16
MnO	0.00	< QL	0.13	< QL	2.12
Na_2O	0.12	0.28	1.36	0.23	14.01
K_2O	0.73	1.00	2.14	0.39	0.25
P_2O_5	0.11	0.11	0.22	< QL	0.05
SO_3	3.09	0.45	0.62	0.17	< QL
LOI	5.41	17.08	7.84	1.54	2.80

*QL= Quantifiable limit LOI = Loss on Ignition

Figure 4. Chemical and mineralogical composition of powders.

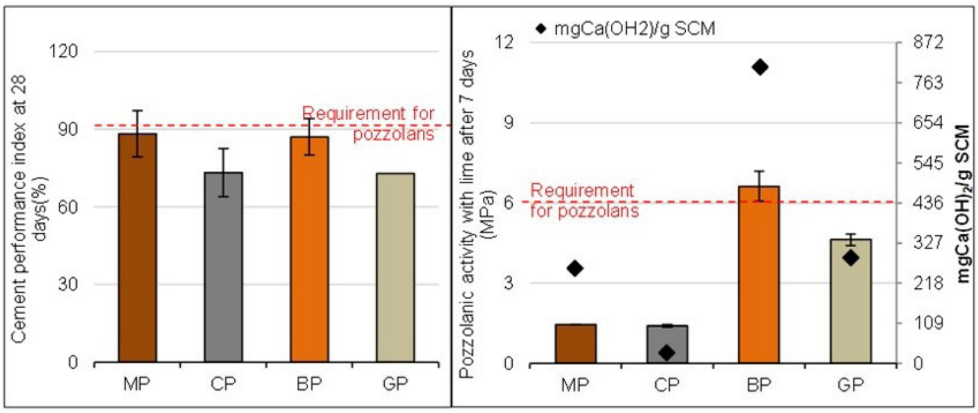

a) Cement performance index b) Activity with lime at 7 days

Figure 5. SCM reactivity.

Oliveira, Dezen, and Possan (2020) also found that concrete powder (CP) acted only as a filler (26). Oliveira et al. (2024) used mixed-origin powders, and even after thermoactivation, they did not obtain pozzolanic activity. Brekailo et al. (2019) analyzed CP and BP using indirect methods and found pozzolanic activity only in BP, while CP behaved more similarly to limestone filler (24).

In this sense, the contribution of ceramic brick powder is related to the development of pozzolanic activity, which affects the chemical reactivity and mechanical strength of the composite, promoting a reaction with calcium hydroxide that generates additional cementitious products and improves the concrete's properties. The pozzolanic activity tends to increase compressive strength, improve durability, and reduce the permeability of concrete, contributing to the longevity of structures. The contribution of the other residues was attributed to the filler effect, which improves the microstructure and reduces the cementitious material's porosity, increasing density and resistance to attack by aggressive agents.

3.2. Concrete PSD and characterization at the fresh state

The particle size distribution (PSD) curves that best fitted Alfred model for the concretes produced with MP, GP, BP and CP are shown in Figure 6. The RSS value for all PSD curves was low, indicating a good proximity of the concrete curves with the target curves achieved using Alfred model.

Regarding the fresh state behavior, the reference concretes designed with q values of 0.17 and 0.27 reached slump test values of 210 and 200 mm, respectively, both within the limits of class S160. However, since a distribution modulus q of 0.17 leads to a greater content of fines in the mixes and we aimed to maximize the use of the SCM, the value of q equal to 0.17 was chosen for the concretes with SCM. The slump test results of these concretes with SCM were also within the limits of class S160, being 200 mm for concrete with MP, 215 mm for concrete with CP, 210 mm for concrete with BP, and 220 mm for concrete with glass powder. Lopes, Peçanha, and Castro (2020) achieved similar value of 213 mm for the slump test for a concrete designed with a distribution modulus of 0.16 (46).

The slump test values obtained in this study differed from the literature since it indicates concretes should be self-compacting when the distribution modulus equals 0.17. This shows that not only the value of the distribution modulus dictates the fresh behavior of concrete, but also some characteristics of the aggregates, such as shape and texture for example. The spherical particles promote greater packing density and contribute to the fluidity of the mixture (70,71); thus, using gravel with angular edges in concrete may have prevented it from being self-compacting.

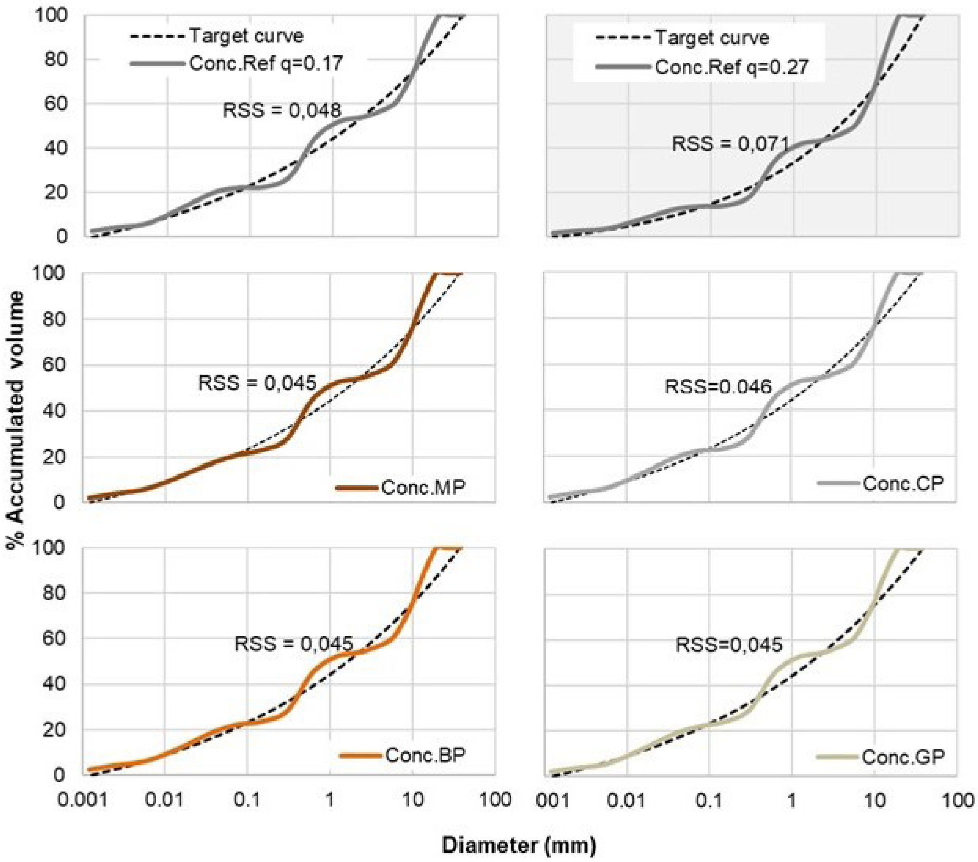

Figure 6. Concrete optimization PSD curves.

3.3. Concrete characterization at the hardened state

Figure 7 presents the compressive strength of concrete at 28 and 180 days. It shows there were no significant gains in mechanical performance between the ages of 28 and 180 days, possibly due to the use of high initial strength Portland cement. On the other hand, there was a significant change in the reference concrete's mechanical strength. The concrete designed with a distribution modulus of 0.17 showed a compressive strength three times higher than the concrete with q=0.27. This is due to the higher content of cement (352 kg/m^3 for concrete REF q=0.27 and 526 kg/m^3 for concrete REF q=0.17, as indicated previously in Table 2). The higher fines content also leads to a better distribution of the paste in the porosity left by the aggregates since this concrete had more fines in its composition and it presented higher slump test value.

When observing the influence of SCM, the 48% replacement of Portland cement with mixed powder was detrimental to mechanical performance, reducing compressive strength by 33% compared to the reference with the same distribution modulus of 0.17. It should be noted that even with the loss of performance, concrete Conc.MP reached 37 MPa. The other concretes, Conc.CP, Conc.BP, and Conc.GP, showed mechanical strength statistically like the reference concrete REF q=0.17, close to 50 MPa.

Oliveira (2022) carried out studies with concrete waste powder, mixed waste powder, and ceramic waste powder, provided by packing techniques as a partial replacement for Portland cement. The concretes produced reached a potential strength at 28 days of 95 MPa for concrete powder, 83 MPa for mixed powder and 63 MPa for brick powder, double the strength compared to the reference (59).

Sales e Alferes Filho (2014) using ceramic waste powder as a partial replacement for Portland cement in concrete, considering 10, 20, and 40% replacements, obtained better compressive performance with a 20% addition (72). Likes et al. (2022) replaced Portland cement with 20% recycled concrete powder mechanically activated by grinding and a 0.43 w/f (water/fines) ratio, obtaining a compressive strength of 36 MPa at 28 days and 40 MPa at 56 days (73).

In this study, for concretes with brick powder, 43% of the cement was replaced by SCM, achieving a strength of 50 MPa, which can be attributed to the pozzolanic activity of the material. Concretes with glass powder and concrete powder, with similar replacement levels of 32% and 33%, respectively, obtained the same mechanical performance, using materials that contribute to the microstructure through the filler effect.

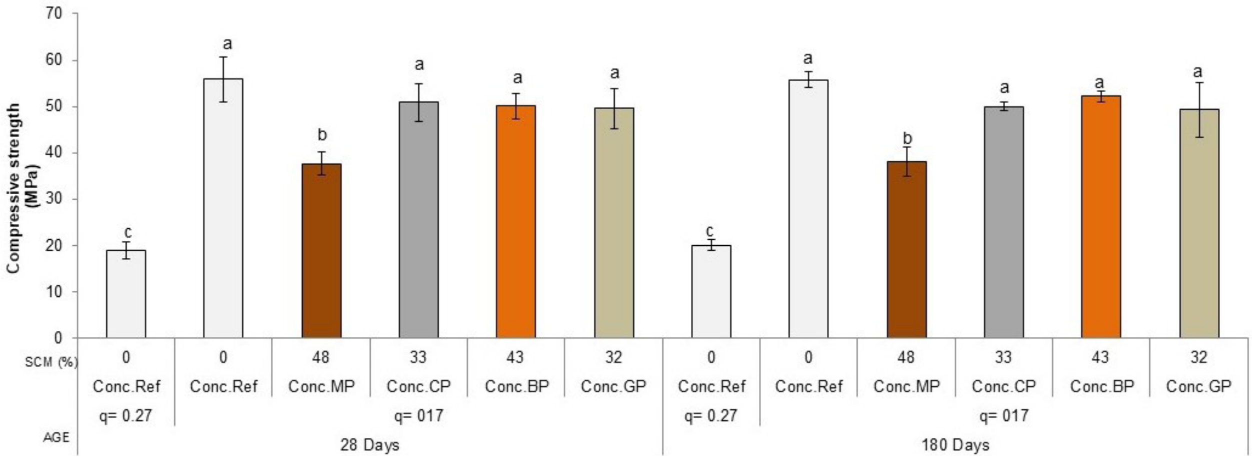

*The letters above the bars indicate the classification according to ANOVA

Figure 7. Compressive strength at 28 days and 180 days.

Physical properties are presented in Figure 8, where results of voids index and absorption are directly proportional, as expected. The concrete with mixed powder had the highest absorption of 5.2%, followed by concrete with ceramic brick powder with 4.9%, both with voids index of approximately 11%. Concrete designed with concrete powder showed absorption and voids index close to the reference Ref q=0.17.

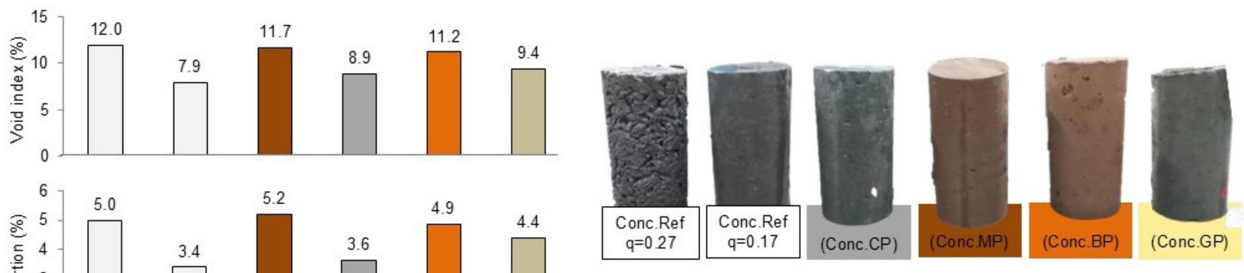

Specific mass (Kg/m³)	q= 0.27	q= 017				
	Conc.Ref	Conc.Ref	Conc.MP	Conc.CP	Conc.BP	Conc.GP
	2.7	2.5	2.5	2.7	2.6	2.4

Figure 8. Absorption, specific mass, and voids index.

All concretes with SCM presented modulus of elasticity lower than the reference concrete Ref q=0.17 (64 GPa) (Figure 9). Concretes with MP and BP showed the highest voids index and the lowest modulus of elasticity, around 40 GPa. On the other hand, concretes with concrete powder and glass powder had similar modulus of elasticity of 55 GPa. The greater the porosity of the material, the lower the modulus of elasticity (74).

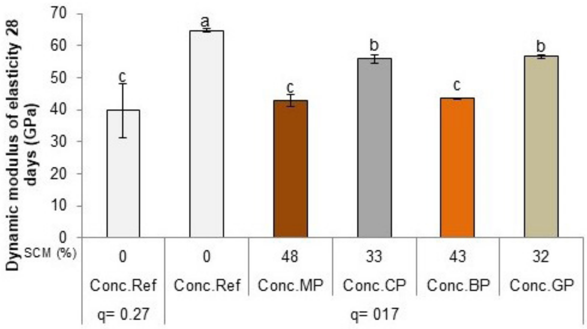

Figure 9. Dynamic modulus of elasticity.

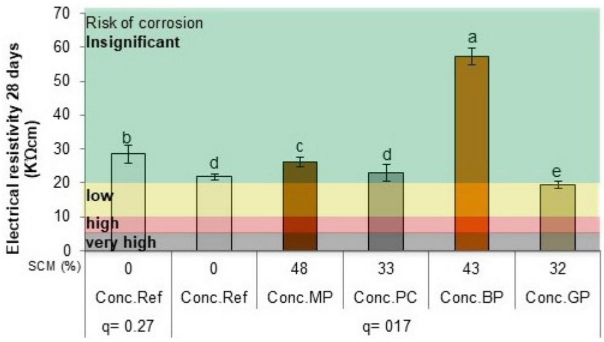

Figure 10. Surface electrical resistivity at 28 days.

Electrical resistivity is associated with the ability to resist the transport of ions subjected to an electric field. It strongly depends on the concrete's microstructure regarding pore size and capillarity. Less permeable concrete has a smaller pore network and, therefore, higher resistivity (77,80). The C-S-H resulting from the pozzolanic reaction blocks the pore network, preventing electric current from passing through, which increases resistivity (81). It could be one of the main reasons for the higher resistivity of concrete with brick powder, replacing 43% of Portland cement. Likes et al. (2022) used ceramic powder to replace 20% of Portland cement and found a 24% increase in electrical resistivity (73). The replacement using glass powder also increased resistivity in the studies by (82,83).

3.4. Environmental indicators for the concretes

As the binder and carbon indexes depend on mechanical performance, the binder index (Figure 11a) follows the same trend as the carbon index (Figure 11b). The best indicators were achieved for concrete with brick powder (5.89 kg/m³ of cement/MPa), and concrete powder (6.94 kg/m³ of cement/MPa). Damineli (2010) suggested a binder index between 10 to 12 kg/m³/MPa for concrete with a strength of up to 50 MPa (84).

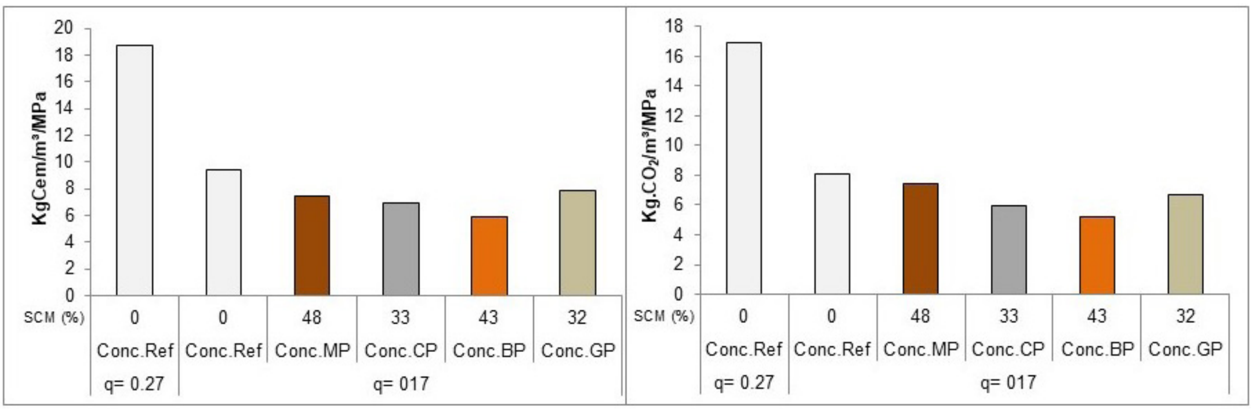

Figure 11. Left: binder index; right: carbon index.

For the carbon index (Figure 11b), the lowest indicators were 5.17 and 5.97 for concrete incorporating 43% and 33% brick and concrete powder, respectively. The worst indicator was associated with MP due to the higher content of mixed powder and the poor mechanical performance, which left this index close to the reference concrete with q=0.17.

The data from this study was compared with Arif et al. (2021), Campos et al. (2022), Liu et al. (2024), Senol and Karakurt (2024), and Soliman (2016) (32,85–88), who showed data on the materials emissions or concrete compositions and compressive strength, as shown in Figure 12.

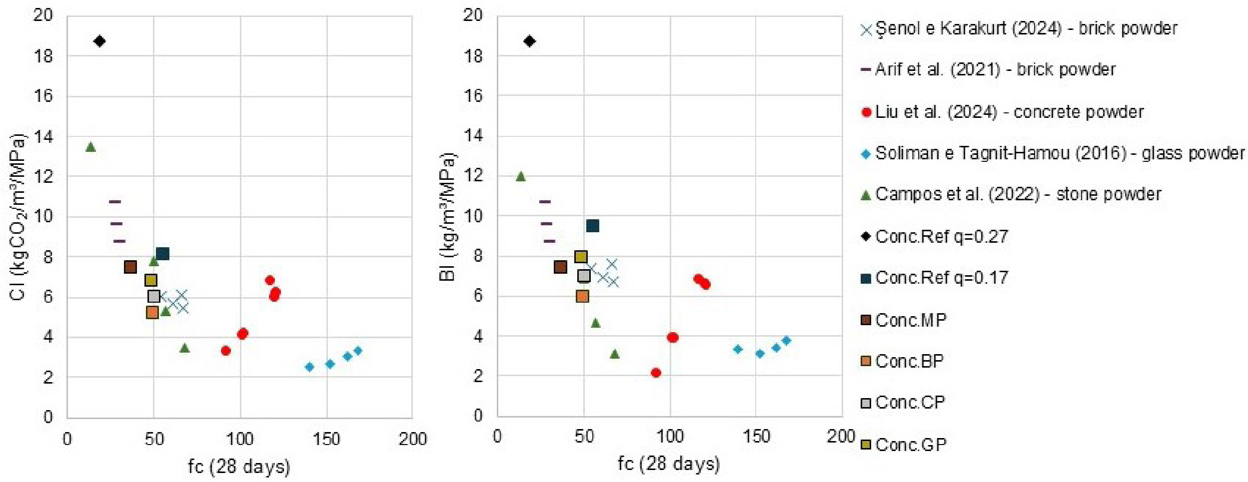

Figure 12. Comparison with the literature on environmental indicators.

The aim was to compare the performance of the developed concretes with others in literature, even though not all concretes presented in Figure 12 were dosed using the Alfred model. It can be observed that the values obtained were relatively lower than those of Arif et al. (87), who used brick powder in the composition and obtained lower mechanical strength. It was noted that for the same 30 - 50 MPa mechanical performance range, the indexes in this study were similar to those of Senol and Karakurt (88) and close to the values obtained by Campos et al. (32). In mechanical strength ranges above 50 MPa, it is seen that the concretes with the highest mechanical performance produced by Liu et al. (86) and Soliman and Tagnit-Hamou (85) had significantly lower carbon and binder indexes than those in this study, as expected since they are ultra-high performance concretes and exceed 100 MPa.

When analyzing concretes with similar compressive strength as the ones obtained in this study, it is noted that the binder index was even lower than those found in the literature, demonstrating the potential to value recycled powders in concrete production as supplementary cementitious materials.

4. CONCLUSIONS

Given the aim of this study to analyze the performance of concretes designed by Alfred model with SCM of different origins, the fallowing main conclusions may be drawn:

a) For the aggregates used in the present study, the concrete mix-design using the modulus of distribution q = 0.17 in Alfred model resulted in concrete with searched behavior in the fresh state (class S160), achieving the highest slump test value among the concretes studied. It also maximized the fines content and, as a result, the Portland cement substitution by SCM, which is desirable in terms of environmental sustainability.
b) The brick powder from CDW ceramic brick proved to be pozzolanic, and this effect may have contributed to the better performance of the concrete containing this SCM. On the other hand, the glass, concrete, and mixed powders had no pozzolanic activity, contributing to the matrix by the filler effect.
c) All concretes presented compressive strength higher than 40 MPa. Furthermore, with the exception of the concrete with mixed powder; all others were considered high-strength, with compressive strength exceeding 50 MPa.
d) The risk of corrosion associated with the electrical resistivity test was insignificant for the concretes in this study containing brick, mixed, and concrete powder (> 20 KΩcm). For concrete containing glass powder, the risk of corrosion was low (between 10 and 20 KΩcm).
e) It was possible to obtain a binder index of 5.89 kg/m³ of cement/MPa and a carbon index of 5.17 kg/m³ of CO_2/MPa for the composition containing 43% brick powder as a replacement for Portland cement.
f) The current study demonstrated the potential value of CDW and glass as powder fractions substituting Portland cement in cementitious matrices with appropriate mix-design techniques. It allows for reduced Portland cement consumption in concrete with performance compatible with structural applications.

Acknowledgements

The authors would like to thank the Instituto Federal do Paraná (IFPR) – Campus Foz do Iguaçu and company Mineromix Concrete. CAPES for their research grant to the author Melissa Pastorini Proença (CAPES code 001), Post-graduation Program in Civil Engineering at the Federal University of Parana (PPGEC/UFPR), and PRPPG/UFPR for their research support.

Authorship contribution statement

Melissa Pastorini Proença: Write-up - original draft, Conceptualization, Research, Methodology Formal analysis, Validation.
Mayara Pastorini Proença: Methodology, Research, Formal analysis.
Miguel Batista de Oliveira: Methodology, Research.
Luis Miguel Zanette Oliveira: Methodology.
Dayana Ruth Bola Oliveira: Conceptualization, Supervision, Write-up - review & editing.
Heloisa Fuganti Campos: Supervision, Write-up - review & editing.
Nayara Soares Klein: Supervision, Write-up - review & editing.

Declaration of competing interests

The authors of this article declare that they have no financial, professional or personal conflicts of interest that could have inappropriately influenced this work.

Data availability

The experimental data obtained in the study could be requested directly from the authors.

REFERENCES

1. Lin Q, Zhang X, Wang T, Zheng C, Gao X. 2022. Technical perspective of carbon capture, utilization, and storage. Engineering. 14:27-32. https://doi.org/10.1016/j.eng.2021.12.013
2. Thomas BS. 2018. Green concrete partially comprised of rice husk ash as a supplementary cementitious material – A comprehensive review. Renew Sustain Energy Rev. 82:3913-3923. https://doi.org/10.1016/j.rser.2017.10.081
3. IEA. 2018. Technology roadmap: Low-carbon transition in the cement industry. París (Francia): International Energy Agency.
4. WBCSD, IEA. 2018. Low carbon technology roadmap for the Indian cement sector: status review 2018. Geneva: World Business Council for Sustainable Development; p. 52.
5. SIDAC. 2024. Dados Do Produto - Clínquer. SIDAC. https://sidac.org.br/produtos/45 (accessed January 8, 2024).
6. SNIC e ABCP. 2019. Roadmap Tecnológico do Cimento. São Paulo (Brasil): Sindicato Nacional da Indústria do Cimento.
7. GCCA. 2022. GNR 2.0 – GCCA in Numbers. Glob. Cem. Concr. Assoc. https://gccassociation.org/innovandi/gccrn/about-innovandi/ (accessed November 19, 2022).
8. Adesina A. 2020. Recent advances in the concrete industry to reduce its carbon dioxide emissions. Environ Challenges. 1:100004. https://doi.org/10.1016/j.envc.2020.100004
9. Sinkhonde D, Bezabih T. 2024. On the computational evaluation of carbon dioxide emissions of concrete mixes incorporating waste materials: A strength-based approach. Clean Waste Syst. 8:100149. https://doi.org/10.1016/j.clwas.2024.100149
10. Jungclaus MA, Williams SL, Arehart JH, Srubar WV. 2024. Whole-life carbon emissions of concrete mixtures considering maximum CO_2 sequestration via carbonation. Resour Conserv Recycl. 206:107605. https://doi.org/10.1016/j.resconrec.2024.107605
11. Tang B, Wu H, Wu Y. 2024. Evaluation of the carbon reduction benefits of adopting the compression cast technology in concrete components production based on LCA. Resour Conserv Recycl. 208:107733. https://doi.org/10.1016/j.resconrec.2024.107733
12. Zhang D. 2024. CO_2 utilization for concrete production: Commercial deployment and pathways to net-zero emissions. Sci Total Environ. 931:172753. https://doi.org/10.1016/j.scitotenv.2024.172753
13. Cembureau. 2021. Activity Report-2020. Bruselas (Bélgica): The European Cement Association.
14. Scrivener KL, John VM, Gartner EM. 2018. Eco-efficient cements: Potential economically viable solutions for a low-CO_2 cement-based materials industry. Cem Concr Res. 114:2-26. https://doi.org/10.1016/j.cemconres.2018.03.015
15. Portland Cement Association (PCA). 2021. Roadmap to carbon neutrality: A more sustainable world is shaped by concrete. Am Cem Manuf. 51:79
16. Skibsted J, Snellings R. 2019. Reactivity of supplementary cementitious materials (SCMs) in cement blends. Cem Concr Res. 124:105799. https://doi.org/10.1016/j.cemconres.2019.105799
17. Snellings R, Suraneni P, Skibsted J. 2023. Future and emerging supplementary cementitious materials. Cem Concr Res. 171:107199. https://doi.org/10.1016/j.cemconres.2023.107199
18. De Matos PR, Sakata RD, Onghero L, Uliano VG, De Brito J, Campos CEM, Gleize PJP. 2021. Utilization of ceramic tile demolition waste as supplementary cementitious material: An early-age investigation. J Build Eng. 38:102187. https://doi.org/10.1016/j.jobe.2021.102187
19. Khan MNN, Saha AK, Sarker PK. 2020. Reuse of waste glass as a supplementary binder and aggregate for sustainable cement-based construction materials: A review. J Build Eng. 28:101052. https://doi.org/https://doi.org/10.1016/j.jobe.2019.101052
20. Lothenbach B, Scrivener K, Hooton RD. 2011. Supplementary cementitious materials. Cem Concr Res. 41:1244-1256. https://doi.org/10.1016/j.cemconres.2010.12.001

21. Oliveira DRB, Leite G, Possan E, Marques Filho J. 2023. Concrete powder waste as a substitution for Portland cement for environment-friendly cement production. Constr Build Mater. 397:132382. https://doi.org/10.1016/j.conbuildmat.2023.132382
22. Kaliyavaradhan SK, Ling T, Mo KH. 2020. Valorization of waste powders from cement-concrete life cycle: A pathway to circular future. J Clean Prod. 268:122358. https://doi.org/10.1016/j.jclepro.2020.122358
23. Frías M, Guerrero A, Monasterio M, Insignares Á, Sánchez MIR. 2024. Viability of using limestone concrete waste from CDW to produce ternary cements type LC3. Constr Build Mater. 411:134362. https://doi.org/10.1016/j.conbuildmat.2023.134362
24. Brekailo F, Pereira E, Pereira E, Filho JH, De Medeiros MHF. 2019. Evaluation of the reactive potential of additions of red ceramic waste and comminuted concrete of CDW in cement matrix. Ceramica. 65:351-358. https://doi.org/10.1590/0366-69132019653752552
25. Robayo-Salazar R, Valencia-Saavedra W, De Gutiérrez RM. 2022. Recycling of concrete, ceramic, and masonry waste via alkaline activation: Obtaining and characterization of hybrid cements. J Build Eng. 46:103698.. https://doi.org/10.1016/J.JOBE.2021.103698
26. Oliveira TCF, Dezen BGS, Possan E. 2020. Use of concrete fine fraction waste as a replacement of Portland cement. J Clean Prod. 273:123126. https://doi.org/10.1016/j.jclepro.2020.123126
27. Proença MP, Oliveira DRB, Risson KDBS, Possan E. 2024. CDW powder activated by mechanical, thermal and tannic acid treatment: an option for circularity in construction. Waste Biomass Valoriz. 16:2367-2390. https://doi.org/10.1007/s12649-024-02802-y
28. Oliveira DRB, Proença MP, Marques Filho J, Possan E. 2024. Mixed construction and demolition powder as a filler to Portland cement: study on packaged pastes. Ambient Construído. 24. https://doi.org/10.1590/s1678-86212024000100715.
29. Jiang X, Xiao R, Bai Y, Huang B, Ma Y. 2022. Influence of waste glass powder as a supplementary cementitious material (SCM) on physical and mechanical properties of cement paste under high temperatures. J Clean Prod. 340:130778. https://doi.org/10.1016/J.JCLEPRO.2022.130778
30. Londero C, Klein NS, Mazer W. 2021. Study of low-cement concrete mix-design through particle packing techniques. J Build Eng. 42:103071.. https://doi.org/10.1016/j.jobe.2021.103071
31. Klein NS, Lenz LA, Mazer W. 2020. Influence of the granular skeleton packing density on the static elastic modulus of conventional concretes, Constr. Build. Mater. 242:118086. https://doi.org/10.1016/j.conbuildmat.2020.118086
32. Campos HF, Bellon AL, Silva ERL, Villatore Junior M. 2022. Eco-efficient concrete, optimized by Alfred's particle packing model, with partial replacement of Portland cement by stone powder, Rev. IBRACON Estruturas e Mater. 15(2):1-14. https://doi.org/10.1590/s1983-41952022000200005
33. Kurda R, Salih A, Shakor P, Saleh P, Alyousef R, Ahmed H, Aslani F. 2022. Mix design of concrete: Advanced particle packing model by developing and combining multiple frameworks, Constr. Build. Mater. 320:126218. https://doi.org/10.1016/j.conbuildmat.2021.126218
34. Funk JE, Dinger DR. 1994. Predictive process control of crowded particulate suspensions. Boston, MA: Springer US. https://doi.org/10.1007/978-1-4615-3118-0
35. ABNT NBR 16697. 2018. Cimento Portland — Requisitos. Associação Brasileira de Normas Técnicas, Río de Janeiro.
36. ABNT NBR 11768-1. 2019. Aditivos químicos para concreto de cimento Portland - Parte 1: Requisitos. Associação Brasileira de Normas Técnicas, Río de Janeiro.
37. Kantro D. 1980. Influence of Water-Reducing Admixtures on Properties of Cement Paste—A Miniature Slump Test. Cem Concr Aggregates. 2(2):95-102. https://doi.org/10.1520/cca10190j
38. ABNT NBR 15116. 2021. Agregados reciclados para uso em argamassas e concretos de cimento Portland - Requisitos e métodos de ensaios. Associação Brasileira de Normas Técnicas, Río de Janeiro.
39. ABNT NBR 5752. 2014. Materiais pozolânicos — Determinação do índice de desempenho com cimento Portland aos 28 dias. Associação Brasileira de Normas Técnicas, Río de Janeiro.
40. ABNT NBR 5751. 2015. Materiais pozolânicos ― Determinação da atividade pozolânica com cal aos sete dias. Associação Brasileira de Normas Técnicas, Río de Janeiro.
41. ABNT NBR 15895. 2010. Materiais pozolânicos – Determinação do teor de hidróxido de cálcio fixado – Método Chapelle modificado. Associação Brasileira de Normas Técnicas, Río de Janeiro.
42. Yu R, Song Q, Wang X, Zhang Z, Shui Z, Brouwers HJH. 2017. Sustainable development of Ultra-High Performance Fibre Reinforced Concrete (UHPFRC): Towards to an optimized concrete matrix and efficient fibre application. J Clean Prod. 162:220-233. https://doi.org/10.1016/j.jclepro.2017.06.017
43. Hunger M. 2010. An integral design concept for ecological self-compacting concrete [PhD thesis]. Eindhoven (Netherlands): Technische Universiteit Eindhoven https://doi.org/10.6100/IR674188
44. Sun Z, Cao S, Xiong J, Zhu J, Liu K, Hu Z. 2023. A nonlinear particle packing model for micro-aggregate. Constr Build Mater. 379:131213. https://doi.org/10.1016/j.conbuildmat.2023.131213
45. Funk JE, Dinger DR. Computer modelling of particle packing phenomena. In: Predictive process control of crowded particulate suspensions. Boston, MA: Springer US; 1994. p. 95–103. https://doi.org/10.1007/978-1-4615-3118-0_8
46. Lopes HMT, Peçanha ACC, De Castro AL. 2020. Considerações sobre a eficiência de misturas de concreto de cimento Portland com base no conceito de empacotamento de partículas. Matéria (Rio Janeiro). 25(1). https://doi.org/10.1590/s1517-707620200001.0874
47. Mercuri E. 2023. Monte Carlo Method for calculating maximum packing density of mixtures, GitHub. 95. https://github.com/emiliomercuri/MixturesMonteCarlo (accessed September 15, 2023).
48. Christófolli JL, Campos HF, Klein NS, Marques Filho J. 2025. Use of high-energy milling for reducing CO_2 emissions in quaternary blends of Portland cement, Constr. Build. Mater. 459: 139470. https://doi.org/10.1016/j.conbuildmat.2024.139470
49. Yu R, Spiesz P, Brouwers HJH. 2014. Mix design and properties assessment of Ultra-High Performance Fibre Reinforced Concrete (UHPFRC), Cem. Concr. Res. 56:29–39. https://doi.org/10.1016/j.cemconres.2013.11.002
50. ABNT NBR 8953. 2015. Concreto para fins estruturais — Classificação pela massa específica, por grupos de resistência e consistência. Río de Janeiro (Brasil): Associação Brasileira de Normas Técnicas.
51. Damineli BL. 2013. Conceitos para formulação de concreto com baixo consumo de ligantes: controle reológico, empacotamento e dispersão de partículas [Tese de doutorado]. São Paulo (Brazil): Universidade de São Paulo.
52. Campos HF. 2019. Dosagem de concreto sustentável e de alta resistência, otimizada por modelos de empacotamento de partículas, com substituição parcial do cimento Portland por pó de pedra e sílica ativa [Tese de doutorado]. Curitiba (Brazil): Universidade Federal do Paraná.
53. ABNT NBR 5738. 2015. Concreto — Procedimento para moldagem e cura de corpos de prova. Associação Brasileira de Normas Técnicas, Río de Janeiro.
54. ABNT NBR 16889. 2020. Concreto — Determinação da consistência pelo abatimento do tronco de cone. Associação Brasileira de Normas Técnicas, Río de Janeiro.
55. ABNT NBR 9778. 2009. Argamassa e concreto endurecidos – Determinação da absorção de água, índice de vazios e massa específica. Associação Brasileira de Normas Técnicas, Río de Janeiro.

56. ABNT NBR 5739. 2018. Concreto — Ensaio de compressão de corpos de prova cilíndricos. Associação Brasileira de Normas Técnicas, Río de Janeiro.
57. AENOR UNE 83988-2. 2014. Durabilidad del hormigón. Métodos de ensayo: determinación de la resistividad eléctrica: parte 2: método de las cuatro puntas o de Wenner. Asociación Española de Normalización y Certificación, Madrid.
58. Damineli BL, Kemeid FM, Aguiar PS, John VM. 2010. Measuring the eco-efficiency of cement use. Cem Concr Compos. 32(8):555-562. https://doi.org/10.1016/j.cemconcomp.2010.07.009
59. Oliveira DRB. 2022. Aproveitamento da fração fina de resíduo de concreto como substituto ao cimento Portland [Tese de doutorado]. Curitiba (Brazil): Universidade Federal do Paraná.
60. SIDAC, Dados Do Produto, 2. 2024. https://sidac.org.br/busca (accessed June 2, 2024).
61. EFCA. 2021. Environmental Product Declaration - Concrete admixtures - Plasticizer and superplasticizer. European Federation of Concrete Admixtures Associations, Brusselss.
62. Higuchi AMD, Marques MGS, Ribas LF, Vasconcelos RP. 2021. Use of glass powder residue as an eco-efficient supplementary cementitious material, Constr. Build. Mater. 304:124640. https://doi.org/10.1016/j.conbuildmat.2021.124640
63. Soliman NA, Tagnit-Hamou A. 2017. Partial substitution of silica fume with fine glass powder in UHPC: Filling the micro gap, Constr. Build. Mater. 139:374–383. https://doi.org/10.1016/j.conbuildmat.2017.02.084
64. Hoppe Filho J, Pires CAO, Leite OD, Garcez MR, Medeiros MHF. 2021. Red ceramic waste as supplementary cementitious material: Microstructure and mechanical properties, Constr. Build. Mater. 296:123653. https://doi.org/10.1016/j.conbuildmat.2021.123653
65. Wang L, Wang J, Wang H, Fang Y, Shen W, Chen P, Xu Y. 2022. Eco-friendly treatment of recycled concrete fines as supplementary cementitious materials, Constr. Build. Mater. 322:126491. https://doi.org/10.1016/J.CONBUILDMAT.2022.126491
66. Wu H, Xiao J, Liang C, Ma Z. 2021. Properties of cementitious materials with recycled aggregate and powder both from clay brick waste, Buildings. 11(3):119. https://doi.org/10.3390/buildings11030119
67. ABNT NBR 12653. 2014. Materiais pozolânicos — Requisitos. Associação Brasileira de Normas Técnicas, Río de Janeiro.
68. Pelisser F, Steiner LR, Bernardin AM. 2012. Recycling of porcelain tile polishing residue in portland cement: Hydration efficiency, Environ. Sci. Technol. 46(4): 2368–2374. https://doi.org/10.1021/es203118w
69. Hoppe Filho J, Pires CAO, Leite OD, Garcez MR, Medeiros MHF. 2021. Red ceramic waste as supplementary cementitious material: Microstructure and mechanical properties, Constr. Build. Mater. 296:123653. https://doi.org/10.1016/j.conbuildmat.2021.123653
70. Kwan AKH, Chan KW, Wong V. 2013. A 3-parameter particle packing model incorporating the wedging effect, Powder Technol. 237:172–179. https://doi.org/10.1016/j.powtec.2013.01.043
71. Kwan AKH, Mora CFA. 2001. Effects of various shape parameters on packing of aggregate particles. Mag Concr Res. 53(2):91–100.
72. Sales ATC, Alferes Filho RS. 2014. Efeito do pó de resíduo cerâmico como adição ativa para o concreto, Ambient. Construído. 14(1):113-125. https://doi.org/10.1590/S1678-86212014000100010
73. Likes L, Markandeya A, Haider MM, Bollinger D, McCloy JS, Nassiri S. 2022. Recycled concrete and brick powders as supplements to Portland cement for more sustainable concrete, J. Clean. Prod. 364:132651. https://doi.org/10.1016/j.jclepro.2022.132651
74. Callister Junior WD, Rethwisch DG. 2016. Ciência e engenharia de materiais: Uma introdução. 9 ed. Rio de Janeiro (Brasil): LTC.
75. Ge Z, Wang Y, Sun R, Wu X, Guan Y. 2015. Influence of ground waste clay brick on properties of fresh and hardened concrete, Constr. Build. Mater. 98:128–136. https://doi.org/10.1016/j.conbuildmat.2015.08.100
76. Cantero B, Bravo M, De Brito J, Del Bosque IFS, Medina C. 2020. Mechanical behaviour of structural concrete with ground recycled concrete cement and mixed recycled aggregate. J Clean Prod. 275:122913. https://doi.org/10.1016/j.jclepro.2020.122913
77. Azarsa P, Gupta R. 2017. Electrical resistivity of concrete for durability evaluation: A Review. Adv Mater Sci Eng. 2017:8453095. https://doi.org/10.1155/2017/8453095
78. Elkey W, Sellevold EJ. 1995. Electrical resistivity of concrete: Supplement. Oslo (Noruega): Norcem A.S.
79. Song HW, Saraswathy V. 2007. Corrosion monitoring of reinforced concrete structures - A review, Int. J. Electrochem. Sci. 2(1):1–28. https://doi.org/10.1016/s1452-3981(23)17049-0
80. Layssi H, Ghods P, Alizadeh AR, Salehi M. 2015. Electrical resistivity of concrete: Concepts, applications, and measurement techniques, Concr. Int. 37(5): 41–46.
81. Rios RT, Lolli F, Xie L, Xie Y, Kurtis KE. 2021. Screening candidate supplementary cementitious materials under standard and accelerated curing through time-series surface resistivity measurements and change-point detection, Cem. Concr. Res. 148:106538. https://doi.org/10.1016/j.cemconres.2021.106538
82. Du H, Tan KH. 2017. Properties of high volume glass powder concrete, Cem. Concr. Compos. 75:22–29. https://doi.org/10.1016/j.cemconcomp.2016.10.010
83. Schwarz N, Cam H, Neithalath N. 2008. Influence of a fine glass powder on the durability characteristics of concrete and its comparison to fly ash, Cem. Concr. Compos. 30(6):486–496. https://doi.org/10.1016/j.cemconcomp.2008.02.001
84. Damineli BL, Kemeid FM, Aguiar PS, John VM. 2010. Measuring the eco-efficiency of cement use, Cem. Concr. Compos. 32(8):555–562. https://doi.org/10.1016/j.cemconcomp.2010.07.009
85. Soliman NA. 2016. Development of ultra-high-performance concrete using glass powder – Towards ecofriendly concrete, Constr. Build. Mater. 125:600–612. https://doi.org/10.1016/j.conbuildmat.2016.08.073
86. Liu X, Liang C, Zhang Z, Zhang Y, Xu J, Ma Z. 2024. Mechanical performance of low-carbon ultra-high performance engineered cementitious composites (UHP-ECC) with high-volume recycled concrete powder, J. Build. Eng. 88:109153. https://doi.org/10.1016/j.jobe.2024.109153
87. Arif R, Khitab A, Kırgız MS, Khan RBN, Tayyab S, Khan RA, Anwar W, Arshad MT. 2021. Experimental analysis on partial replacement of cement with brick powder in concrete, Case Stud. Constr. Mater. 15:e00749. https://doi.org/10.1016/j.cscm.2021.e00749
88. Şenol AF, Karakurt C. 2024. High-strength self-compacting concrete produced with recycled clay brick powders: Rheological, mechanical and microstructural properties, J. Build. Eng. 88:109175. https://doi.org/10.1016/j.jobe.2024.109175